Programmed Two-Dimensional Self-Assembly of Multiple DNA Origami Jigsaw Pieces

Arivazhagan Rajendran,[†,‡] Masayuki Endo,*[,‡,§] Yousuke Katsuda,[†] Kumi Hidaka,[†] and Hiroshi Sugiyama*[,†,‡,§]

[†]Department of Chemistry, Graduate School of Science, Kyoto University, Kitashirakawa-oiwakecho, Sakyo-ku, Kyoto 606-8502, Japan, [‡]CREST, Japan Science and Technology Corporation (JST), Sanbancho, Chiyoda-ku, Tokyo 102-0075, Japan, and [§]Institute for Integrated Cell-Material Sciences (iCeMS), Kyoto University, Yoshida-ushinomiyacho, Sakyo-ku, Kyoto, 606-8501, Japan

ABSTRACT We demonstrate a novel strategy of self-assembly to scale up origami structures in two-dimensional (2D) space using multiple origami structures, named "2D DNA jigsaw pieces", with a specially designed shape. For execution of 2D self-assembly along the helical axis (horizontal direction), sequence-programmed tenon and mortise were introduced to promote selective connections *via* π-stacking interaction, sequence-complementarity, and shape-complementarity. For 2D self-assembly along the helical side (vertical direction), the jigsaw shape-complementarity in the top and bottom edges and the sequence-complementarity of single-stranded overhangs were used. We designed and prepared nine different jigsaw pieces and tried to obtain a 3 × 3 assembly. The proof of concept was obtained by performing the assembly in four different ways. Among them, the stepwise self-assembly from the three vertical trimer assemblies gave the target 2D assembly with ~35% yield. Finally, the surfaces of jigsaw pieces were decorated with hairpin DNAs to display the letters of the alphabet, and the self-assembled 2D structure displayed the word "DNA JIG SAW" in nanoscale. The method can be expanded to create self-assembled modules carrying various functional molecules for practical applications.

KEYWORDS: DNA origami · programmed 2D self-assembly · jigsaw pieces · nanotechnology · fast-scanning atomic force microscopy

The unique structural motifs and molecular recognition properties of DNA make it a promising template for building nanostructures.[1−4] Using a long single-stranded DNA as a template, a novel strategy, the so-called DNA origami method, has been developed for the preparation of various two-dimensional (2D) and three-dimensional (3D) nanostructures with defined size.[5−12] In addition, these origami nanostructures have been used as a platform for the nanopatterning of proteins, nanoparticles, transition metals, and other functional components into deliberately designed arrangements.[13−20] They can also act as templates for the growth of nanowires, aid in the structural determination of proteins, and provide new platforms for genomic applications.[21] However, these structures offer a relatively small area, which is not sufficient for the precise positioning of functional molecules, and a larger assembly with a size of a few micrometers is required for the preparation of practical devices. For instance, conventional photolithography techniques require a size domain of 1 μm. Although programmed DNA and RNA assemblies with the size of around 10−20 nm have been achieved,[22−24] strategies for the construction of defined larger assemblies are limited.

The size of the origami was first expanded by Rothemund with the assembly of triangular origami into a hexagon with a yield of <2%.[5] Later, 3D heterotrimers in the shape of a wireframe icosahedron were reported with no information about the yield of the assembled structures.[10] We have recently developed a new method to scale up DNA origami using jigsaw pieces (JPs) and successfully prepared a unidirectional DNA assembly.[25] However, the 2D construction of origami tiles is critical for the development of DNA origami technology. The 2D scale-up of the origami structure was recently initiated using small DNA tiles with a size of 16 nm ×17 nm as folding staples.[26] Apart from these examples, there is no report for the preparation of larger origami structures (particularly 2D structures), and hence the development of new methods with added advantages is urgently required.

In this work, we demonstrate a new route for the 2D extension of DNA origami using multiple JPs by programmed self-assembly, the spontaneous association of components into organized 2D structures using noncovalent interactions. By altering the shape of our previous origami structure,[25] we have designed nine different JPs, each of which is a 24-helix tile (Figure 1A), containing (i) sequence-programmed connection sites, a tenon, and corresponding mortise, to allow assembly along the

*Address correspondence to hs@kuchem.kyoto-u.ac.jp (H.S.) or endo@kuchem.kyoto-u.ac.jp (M.E.).

Received for review November 22, 2010 and accepted December 13, 2010.

Published online December 28, 2010.
10.1021/nn1031627

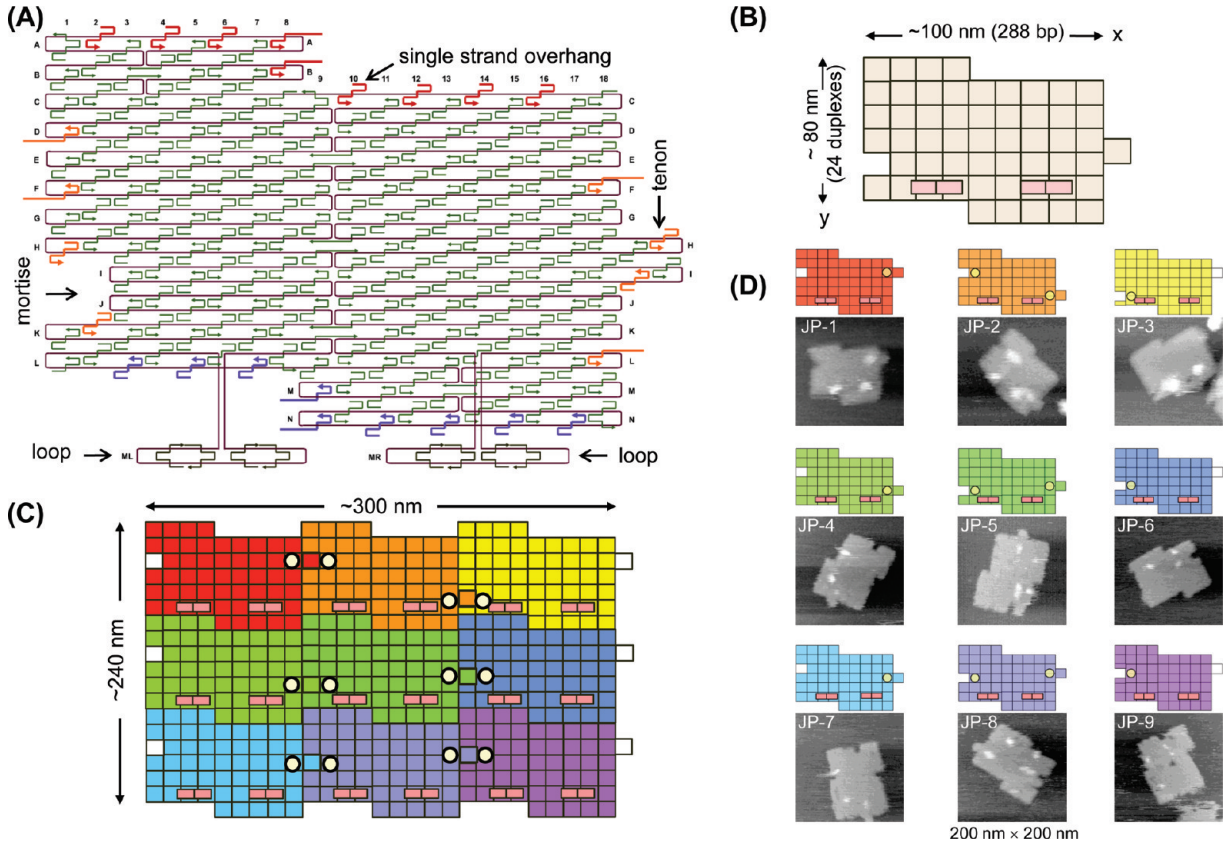

Figure 1. Schematic drawing of the "DNA jigsaw pieces (JPs)", desired self-assembled 2D structure, and the AFM images of the monomer JPs. (A) A model structure of the designed DNA JP having a mortise and a tenon (JP-5). (B) Scheme of the JP-5 represented as a matrix of blocks. One block represents four 32-mer duplexes. (C) Scheme of the desired final structure of the self-assembly. Pink blocks at the bottom of each JP represent the loops. Circles denote the set of four individual hairpin markers. (D) Scheme of the nine monomer JPs showing the position of the tenon, the mortise, and the hairpin markers along with their AFM images.

helical axis (*x*-direction) with the adjacent JP *via* these adhesive connections; (ii) two single-stranded overhangs were kept at the sides of each monomer to make the binding stronger along the helical axis; (iii) protruding single-stranded overhangs have been placed at the bottom side for the first row JPs, the top side for the last row, and both sides for the middle row that base pair with the M13mp18 viral DNA in the neighboring JP to facilitate assembly along the helical side (*y*-direction). In addition to the single-stranded overhangs, jigsaw shapes at the top and bottom sides of each origami structure were created to promote the assembly. The individual monomers were differentiated by changing the position of the tenon and the mortise and also the sequences at the bottom. Two loops at the bottom of each JP were purposely introduced so that the sequence difference between the monomers can be made at the bottom side by adjusting the sequences in the loop. This arrangement is important for the monomers to assemble exclusively with their respective partner. Note that these loops are duplexes containing double-crossovers formed by the portion of the viral DNA with their complementary staple strands. For the identification of each monomer, a set of hairpin DNA strands (each set contains four individual hairpins) was introduced as markers that were adjacent to the tenon and the mortise. To avoid the intertile π-stacking among the same JP monomer, tetrathymidine (T4) units were introduced at both of the side edges of each monomer JP. The size of the monomer was designed to be ~80 nm ×100 nm. A model JP and the expected 2D self-assembled origami structure are shown in Figure 1A−C. The detailed design of the DNA JPs and the sequences of the staple strands are given in the Supporting Information.

RESULTS AND DISCUSSION

The monomer origami JPs were prepared separately by mixing the M13mp18 viral DNA and their respective staple strands in Tris buffer (pH 7.6) containing Mg^{2+} and EDTA. The solution was annealed from 85 to 15 °C at a rate of −1.0 °C/min. The formed DNA piece monomers were deposited on a mica surface and imaged in the liquid using an atomic force microscopy (AFM). The AFM images and the schematic drawing of the monomer JPs represented by the matrix of blocks are given in Figure 1D. The JPs were formed as designed. The size of the JPs in the AFM image is consistent with the original design. The tenon, counterpart mortise, hairpin markers, and the loops at the bottom were observed clearly and were identified in the predesigned places on the jigsaw planar structure. The set of

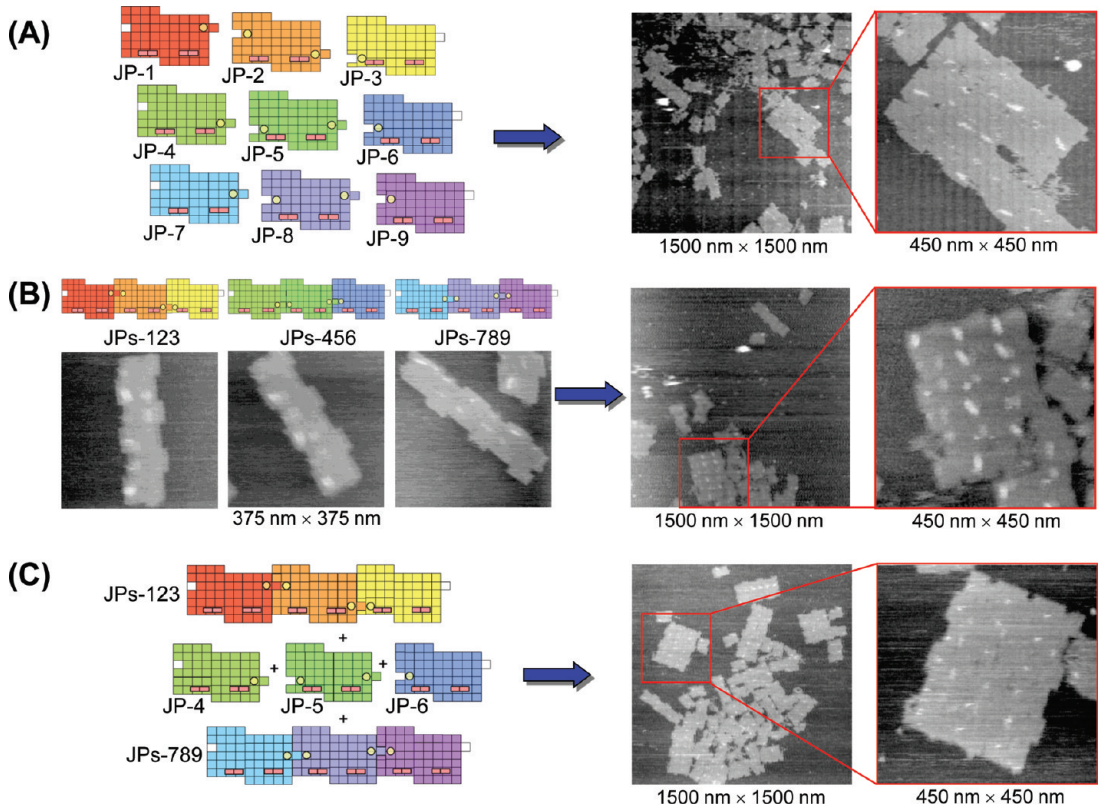

Figure 2. (A) AFM image of the 2D self-assembled structure after nonlinear annealing of the mixture of monomer JPs. (B) AFM images of the trimers self-assembled along the helical axis (left). Schematic drawings of the trimers are shown above the AFM images. The self-assembled final structure prepared from the preassembled trimers (middle and right). (C) Structure of the final product self-assembled from the first and last row trimers and middle row monomers. The right image is an expanded image of the portion of the middle or left image given in the square box. The image sizes are shown below each image.

hairpin markers was placed adjacent to the mortises and the tenons that were involved in the self-assembly, while the marker is not introduced near the tenons and the mortises that were not involved in the assembly process, for instance, the mortises at JPs 1, 4, and 7 and the tenons at JPs 3, 6, and 9. As designed, there are two sets of markers (light spots) on JPs 2, 5, and 8, while there is only one on the rest of the JPs. Two bright spots on the bottom of each JP represent the loops. It is worth mentioning here that the staple strands on the tenon region of JPs 3, 6, and 9 were not added, as they were not designed to make any connection with the neighboring JP during the self-assembly. Hence, the tenons on these JPs in the AFM images do not appear clearly. In addition, the mortises of JPs 1, 4, and 7 were protected from interaction with other JPs by adding four T8 single-stranded overhangs at each mortise.

Before the self-assembly process, the individual monomers were separately passed through a gel-filtration column to remove the excess staple strands. After purification, the monomers were mixed together in equal ratio and the solution was annealed linearly from 50 to 15 °C at various cooling rates, ranging from −0.1 to −0.01 °C/min. From our previous studies,[25] we have noted that the JPs are stable at 50 °C, and the self-assembly is efficient at a slow cooling rate, such as −0.1 or −0.05 °C/min; hence we have used these annealing conditions. AFM imaging of the resulting sample showed that self-assembly with the desired structure was not successfully obtained. We believed that this problem could be solved by optimizing the annealing conditions and adopted the nonlinear condition from 50 to 15 °C by decreasing the temperature by 10 °C and increasing it by 5 °C at a rate of ±0.2 °C/min. The AFM image of the resulting structure is given in Figure 2A. As we expected, the nonlinear annealing condition successfully yielded the 2D self-assembled structure with little damage. The correct orientation of the JPs in the assembled structure is confirmed by the position of the markers. Although the 2D assembled structure was prepared by this method, the yield for monomer conversion was about 10% (Table 1). This low yield is logical because in a reaction with more components (in the present case there are nine components), the overall yield would be low.

Because the yield of two-step self-assembly (the first step is monomer formation, and the second is 2D self-assembly) is low, we decided to make it by three steps: (i) monomer formation as described before; (ii) formation of trimers along the row; and (iii) self-assembly of preassembled trimers. In this method, the number of components in every step would be fewer,

TABLE 1. Comparison of the Yields of the Trimers and the Final Self-Assembled Structures with Different Assembling and Annealing Methods[a]

		yield (%)	
assembly methods	annealing	trimers (1 × 3 or 3 × 1)	final structure (3 × 3)
just by mixing all JPs	linear		0
	nonlinear		<10
horizontal trimers	linear	all ~35 [first: 77, middle: 65, and last: 120]	~10
	nonlinear	~45 [first: 53 and last:47] ~25 [middle: 51]	
horizontal trimers (top and bottom rows) + monomers (middle row)	nonlinear (trimers) linear (final assembly)	~45 [first: 53 and last: 47]	~10
vertical trimers	linear	all ~43 [first: 139, middle: 87, and last: 79]	~35 [52]

[a]The numbers given in the square bracket represent the number of JPs counted to determine the yield.

and thus a better yield is expected. The JPs in the respective row (horizontal assembly; for example, JPs 1, 2, and 3 in the first row) were mixed and annealed linearly from 50 to 15 °C at a rate of −0.1 °C/min. After annealing, the self-assembled trimers were captured in the AFM image (Figure 2B left) and were formed as designed. The yield for the monomer conversion and the size of the trimers were found to be ~35% (Table 1) and 85 nm ×365 nm, respectively. Next, the trimers were mixed together, and the third step annealing, was performed by the same annealing procedure that was used for the trimer formation. The 2D structure was formed as expected (Figure 2B right). However, there was no significant change in the yield of the final structure, and this method resembles the previous case. Moreover, there was a little damage in the formed 2D structure, and this damage might occur due to various reasons, such as problems in the annealing conditions, adsorption of such a large structure onto the mica surface, and mechanical tip effect during the AFM imaging. The observed lower yield might be due to the single-stranded overhangs that were introduced to facilitate the self-assembly along the helical side. These single strands could possibly display undesired nonspecific interactions with other JPs or the trimer assembly and lead to aggregation, as observed in the AFM image (data not shown). Thus, these single strands may not be effectively available for the assembly along the helical side, and hence the yield of the final product was low.

Besides the linear annealing procedure, we have also tried a nonlinear annealing condition to make the trimers along the row. The monomers were annealed from 50 to 15 °C by decreasing the temperature by 10 °C and then increasing it by 5 °C at a rate of ±1.0 °C/min. The yield of the first row and last row trimers was ~45%, while it was ~25% for the middle row (Table 1). This lower yield of the middle row trimer might be due to the presence of single-stranded overhangs at both top and bottom sides, while it was placed only at either side for the other trimers. By taking advantage of the yield of the top and bottom row trimers, we have tried to prepare the 2D assembly by annealing these trimers along with the middle row monomers (JPs 4, 5, and 6). The solution was annealed linearly from 50 to 15 °C at a rate of −0.1 °C/min. The observed structure in the AFM image is shown in Figure 2C. Unlike the previous cases, the 2D self-assembled structure formed without any damage. However, no improvement in the yield was observed.

The results described above clearly show that the single-stranded overhangs at the top and bottom sides of the JPs are highly sensitive and hence need to be protected before the 2D self-assembly. This can be done by hybridizing the single-stranded overhangs with their complementary bases in the neighboring JP. In other words, the trimer formation along the helical side (vertical assembly; for example, JPs 1, 4, and 7) can protect the single-stranded overhangs during the trimer formation, and then the 2D self-assembly can be further carried out. Trimer formation and the consequent 2D self-assembly were performed by linear annealing from 50 to 15 °C at a rate of −0.05 °C/min. Images of the formed trimers are given in Figure 3A. The yield for the monomer conversion and the size of the trimers were ~43% (Table 1) and 260 nm × 120 nm, respectively. Successive annealing yielded the final product, which was confirmed by the clear AFM image shown in Figure 3B. The size of the self-assembled structure is 260 nm × 365 nm, which is consistent with the predesigned structure. The correct orientation of the JPs in the assembled structure was confirmed by the position of the markers (light spot) and the loops (bright spot). In fact, the four individual hairpins in every set of markers were clearly visible in the AFM image. Interestingly, the yield was improved by this method and was found to be ~35% for the monomer conversion (Figure S1 and Table 1). This higher yield confirms our assumption that the single-stranded overhangs need to be protected to avoid aggregation and to get a better yield of the self-assembled product. This is the most interesting possible explanation for the yield increase, because two horizontal trimers bond by 54 strands (9 strands per JP × 3 JPs in a horizontal assembly × 2 trimers) while only 24 between two vertical assemblies [(2 strands at tenon/mortise + 2 overhangs) × 3 JPs in a vertical assembly × 2 trimers]. If nonspecific

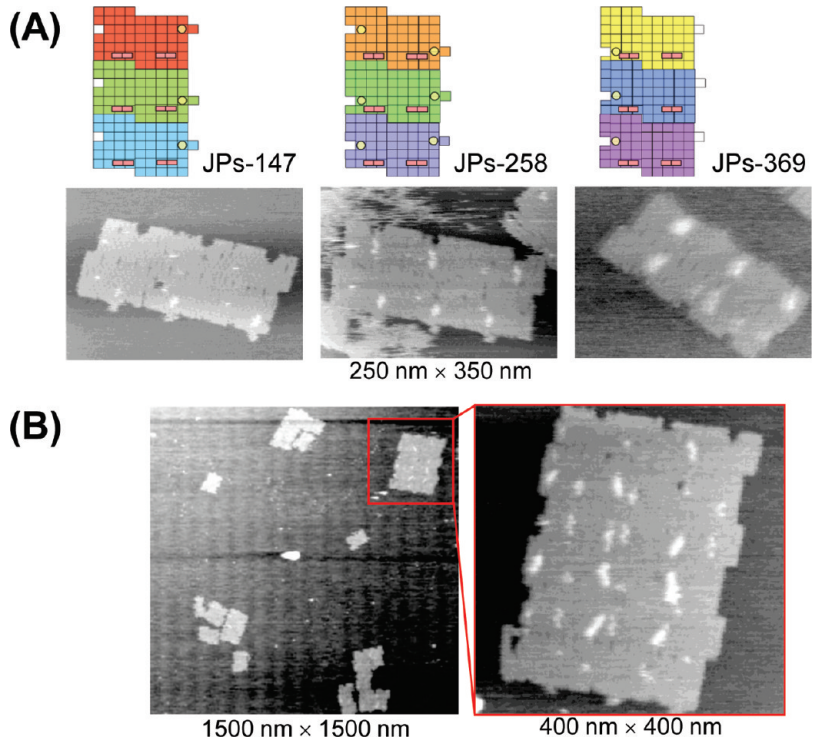

Figure 3. AFM images of the trimers and the 2D self-assembled structure. (A) The structure of the trimers self-assembled along the helical side. Schematic drawings of the trimers are shown along with the AFM images. (B) The self-assembled structure prepared from the preassembled trimers. The bright spots in the image represent the loops at the bottom of each monomer. The light spots represent the hairpin markers, which are adjacent to the tenons and the mortises. The image sizes are shown below each image.

interactions are what is causing the poor yield, then having 54 strands would more likely yield more nonspecific interactions than having 24 strands. This is further evidenced from a slightly better yield (~43%) of the vertical trimers than the horizontal one (~35%). In addition to the nonspecific interactions, there may be a shape-fitting factor, which can also affect the yield of the final assembly. Mortises and the tenons of the vertical trimers do not match up if the wrong vertical trimers bind. In this case, the jigsaw shapes actually could keep incorrect trimers from binding and could give a better yield of the final structure. In the horizontal trimer this is not the case, as every trimer matches the shape of every other horizontal trimer and may lead to a poor yield. Apart from the nonspecific interactions and the shape of the JPs, we should also consider the orientation of the bonds between the helical axis and helical side. In the helical side case there is repulsion between the long edges of the DNA origami that may give this situation a different binding energy than the end-on case, where the π-stacking attractions could lead to a better binding. Besides the assembly methods, the JP monomers are expected to have a slightly twisted structure in solution, because the origami structures were designed to have 10.66 base pairs per turn. This twisted structure may complicate the self-assembly and culminate to the lower overall yield.

Regarding the annealing condition for the 1D (trimer formation) and the 2D assembly, we have tried several conditions ranging from −0.2 to −0.01 °C/min. The best linear condition lies in the range −0.2 to −0.05 °C/min, and a slow annealing rate, such as −0.01 °C/min, leads to aggregation.

Finally, the self-assembled structure was used as a platform for displaying nanoscale words. We built the words "DNA JIG SAW" from the alphabet letters formed by hairpin DNAs on the individual JP. For clear visualization of the letters, the hairpin markers that were placed near the tenons and the mortises were removed. In addition, the staple strands at the loop regions were not added. The monomers with the letters and the self-assembled product carrying the words were prepared by the method described in the previous section (Figure 3). After the first annealing step, we clearly observed the letters on the respective JPs (Figure 4A). The 2D self-assembly by three-step annealing yielded the programmed words on the 2D structure, as shown in the AFM image (Figure 4B). The letters by hairpin markers affect neither the formation, shape, and the yield of the JP monomers nor the 2D self-assembled structure (Figure S2). This suggests that our method may be suitable for the programmed self-assembly of prefunctionalized DNA nanoconstructs to achieve functional nanomaterials.

The strategy we have demonstrated here has high potential for the preparation of 2D DNA assemblies of multiple DNA piece monomers. The designed JPs assembled preferentially *via* the defined connections in a

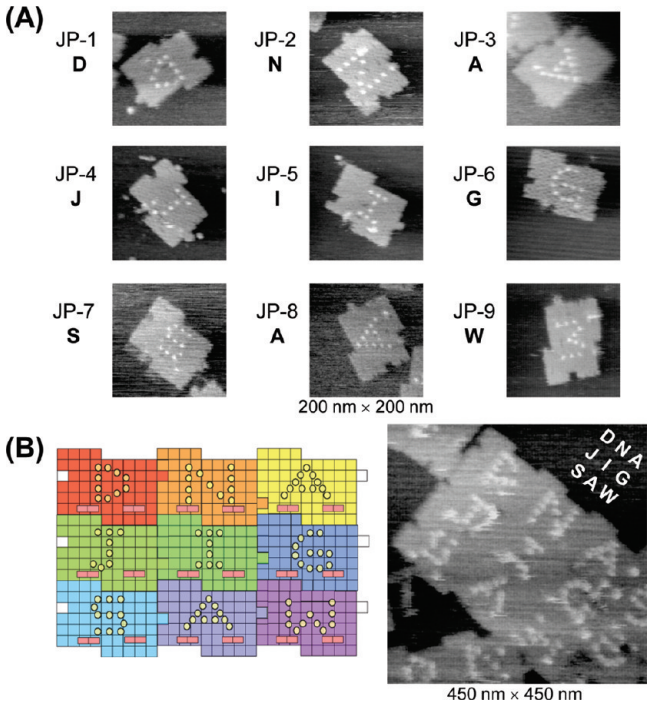

Figure 4. The JPs and the assembled structure displaying letters and words, respectively. (A) The jigsaw piece monomers carrying the letters of the alphabet formed by hairpin DNAs. (B) Schematic drawing and the AFM image of the self-assembled structure carrying the words "DNA JIG SAW". The image sizes are shown below each image.

"lock-and-key" fashion. The mortises, tenons, and the single-stranded overhangs worked efficiently to facilitate the 2D assembly. In particular, the sequence difference made at the bottom of each JP helped to assemble each DNA piece monomer with their respective partner along the helical side. Moreover, the single-stranded overhangs in a JP directly hybridized with the viral DNA in the neighboring piece, which enables assembly without an intertile gap or empty space. Similarly, a tight binding occurs at the sequence-programmed tenons and the mortises. The shape of the side edge and the position of the mortises and the tenons worked not only for the selective connection but also for the exclusion of incorrect connections during self-assembly along the helical axis. In the present study, we have added tetrathymidine (T4) units at the side edges of each monomer, the same as in the case of 1D JP assembly.[25] Even then, the assembly along the helical axis was not prevented, which explains the effectiveness of the mortises and the tenons. The yield of the 2D structure may be further improved by optimizing the annealing procedures based on the thermodynamic parameters of the staple strands and by using different lengths of the single-stranded overhangs. The idea of using jigsaw shapes to increase the specificity of DNA origami interactions and thus increase the yield of assembled origami structures could be verified by using nonjigsaw monomers. Such experiments are under investigation.

CONCLUSIONS

In conclusion, we have demonstrated a novel strategy for the preparation of 2D DNA assemblies by the programmed self-assembly of multiple DNA JPs. The designed jigsaw monomers assembled preferentially *via* the defined connections in a "lock-and-key" fashion after various annealing procedures. The mortises, tenons, and the single-stranded overhangs worked efficiently to promote the 2D assembly. For a better yield, the single-stranded overhangs needed to be hybridized before the 2D self-assembly. The structure that we have prepared is about 3.5 times larger in area than the previously reported structure[26] and is the origami structure with the largest area ever prepared. We anticipate that this method could be successfully applied and extended to build an even larger structure, reaching a size of a few micrometers. The monomers we have taken for the self-assembly use the full length of the M13mp18 viral DNA, which provides enough space for the nanopatterning of various functional molecules, and we expect that the method described here could be expanded for the self-assembly of prefunctionalized origami nanoblocks for practical applications.

MATERIALS AND METHODS

Materials. Tris-HCl, EDTA, and $MgCl_2$ were purchased from Nacalai Tesque, Inc. (Kyoto, Japan). Single-stranded M13mp18 DNA was obtained from New England Biolabs, Inc. (Ipswich, MA, USA, catalog number: #N4040S). The staple strands (most of them are 32-mer) were received from Sigma Genosys (Hokkaido, Japan). The gel-filtration column and the Sephacryl S-300 were purchased from Bio-Rad Laboratories, Inc. (Hercules, CA, USA) and GE Healthcare UK Ltd. (Buckinghamshire, UK), respectively. Water was deionized (≥18.0 MΩ cm specific resistance) by a Milli-Q system (Millipore Corp., Bedford, MA, USA). The hairpin marker sequence used was 5′-TCCTCTTTTGAGGAACAAGTTTTCTTGT-3′.

Preparation of the Monomer Origami Tiles and Self-Assembly. Each JP was prepared by annealing the solution of 0.01 μM M13mp18 DNA, 0.04 μM of each staple DNA strand (4 equiv), 20 mM Tris-HCl (pH 7.6), 1 mM EDTA, and 10 mM $MgCl_2$ from 85 to 15 °C at a rate of −1.0 °C/min. The samples were purified using a Sephacryl S-300 gel-filtration column. The purified monomers were then used for the trimer assemblies and the 2D self-assembly as described in the text.

AFM Imaging. AFM images were obtained using a fast-scanning AFM system (Nano Live Vision, RIBM Co. Ltd., Tsukuba, Japan) with a silicon nitride cantilever (resonant frequency = 1.0−2.0 MHz, spring constant = 0.1−0.3 N/m, EBDTip radius < 15 nm, Olympus BL-AC10EGS-A2). The sample (2 μL) was adsorbed onto a freshly cleaved mica plate (⌀ 1.5 mm, RIBM Co. Ltd., Tsukuba, Japan) for 5 min at room temperature and then washed several times using the same buffer solution. Scanning was performed using the tapping mode in the same buffer solution. The yield of the final structures is given as the fraction of monomers that end up in a complete 3 × 3 (2D self-assembly) or complete 1 × 3/3 × 1 (trimers) structure. The experiments were repeated twice or thrice to get a statistically significant yield.

Acknowledgment. This work was supported by the Core Research for Evolutional Science and Technology (CREST) of JST and a Grant-in-Aid for Science Research from MEXT, Japan.

Supporting Information Available: Additional AFM images, design of the JPs, and staple strand sequences. This material is available free of charge *via* the Internet at http://pubs.acs.org.

REFERENCES AND NOTES

1. Niemeyer, C. M.; Mirkin, C. A., Eds. *Nanobiotechnology: Concepts, Applications and Perspectives*; Wiley-VCH,: Weinheim, Germany, 2004.
2. Seeman, N. C. DNA in a Material World. *Nature* **2003**, *421*, 427–431.
3. Feldkamp, U.; Niemeyer, C. M. Rational Design of DNA Nanoarchitectures. *Angew. Chem., Int. Ed.* **2006**, *45*, 1856–1876.
4. Endo, M.; Sugiyama, H. Chemical Approaches to DNA Nanotechnology. *ChemBioChem.* **2009**, *10*, 2420–2443.
5. Rothemund, P. W. K. Folding DNA to Create Nanoscale Shapes and Patterns. *Nature* **2006**, *440*, 297–302.
6. Andersen, E. S.; Dong, M.; Nielsen, M. M.; Jahn, K.; Subramani, R.; Mamdouh, W.; Golas, M. M.; Sander, B.; Stark, H.; Oliveira, C. L.; Pedersen, J. S.; Birkedal, V.; Besenbacher, F.; Gothelf, K. V.; Kjems, J. Self-Assembly of Nanoscale DNA Box with a Controllable Lid. *Nature* **2009**, *459*, 73–76.
7. Kuzuya, A.; Komiyama, M. Design and Construction of a Box-Shaped 3D-DNA Origami. *Chem. Commun.* **2009**, 4182–4184.
8. Ke, Y.; Sharma, J.; Liu, M.; Jahn, K.; Liu, Y.; Yan, H. Scaffolded DNA Origami of a DNA Tetrahedron Molecular Container. *Nano Lett.* **2009**, *9*, 2445–2447.
9. Endo, M.; Hidaka, K.; Kato, T.; Namba, K.; Sugiyama, H. DNA Prism Structures Constructed by Folding of Multiple Rectangular Arms. *J. Am. Chem. Soc.* **2009**, *131*, 15570–15571.
10. Douglas, S. M.; Dietz, H.; Liedl, T.; Högberg, B.; Graf, F.; Shih, W. M. Self-Assembly of DNA into Nanoscale Three-Dimensional Shapes. *Nature* **2009**, *459*, 414–418.
11. Dietz, H.; Douglas, S. M.; Shih, W. M. Folding DNA into Twisted and Curved Nanoscale Shapes. *Science* **2009**, *325*, 725–730.
12. Ke, Y.; Douglas, S. M.; Liu, M.; Sharma, J.; Cheng, A.; Leung, A.; Liu, Y.; Shih, W. M.; Yan, H. Multilayer DNA Origami Packed on a Square Lattice. *J. Am. Chem. Soc.* **2009**, *131*, 15903–15908.
13. Chhabra, R.; Sharma, J.; Ke, Y.; Liu, Y.; Rinker, S.; Lindsay, S.; Yan, H. Spatially Addressable Multiprotein Nanoarrays Templated by Aptamer-Tagged DNA Nanoarchitectures. *J. Am. Chem. Soc.* **2007**, *129*, 10304–10305.
14. Ke, Y.; Lindsay, S.; Chang, Y.; Liu, Y.; Yan, H. Acid Probe Tiles for Label-Free RNA Hybridization Assays. *Science* **2008**, *319*, 180–183.
15. Sharma, J.; Chhabra, R.; Andersen, C. S.; Gothelf, K. V.; Yan, H.; Liu, Y. Toward Reliable Gold Nanoparticle Patterning on Self-Assembled DNA Nanoscaffold. *J. Am. Chem. Soc.* **2008**, *130*, 7820–7821.
16. Rinker, S.; Ke, Y.; Liu, Y.; Chhabra, R.; Yan, H. Self-Assembled DNA Nanostructures for Distance-Dependent Multivalent Ligand-Protein Binding. *Nat. Nanotechnol.* **2008**, *3*, 418–422.
17. Shen, W.; Zhong, H.; Neff, D.; Norton, M. L. NTA Directed Protein Nanopatterning on DNA Origami Nanoconstructs. *J. Am. Chem. Soc.* **2009**, *131*, 6660–6661.
18. Gu, H.; Chao, J.; Xiao, S.; Seeman, N. C. Dynamic Patterning Programmed by DNA Tiles Captured on a DNA Origami Substrate. *Nat. Nanotechnol.* **2009**, *4*, 245–248.
19. Maune, H. T.; Han, S.; Barish, R. D.; Bockrath, M.; Goddard, W. A., III; Rothemund, P. W. K.; Winfree, E. Self-assembly of Carbon Nanotubes into Two-Dimensional Geometries Using DNA Origami Templates. *Nat. Nanotechnol.* **2010**, *5*, 61–66.
20. Voigt, N. V.; Torring, T.; Rotaru, A.; Jacobsen, M. F.; Ravnsbak, J. B.; Subramani, R.; Mamdouh, W.; Kjems, J.; Mokhir, A.; Besenbacher, F.; Gothelf, K. V. Single-Molecule Chemical Reactions on DNA Origami. *Nat. Nanotechnol.* **2010**, *5*, 200–203.
21. Douglas, S. M.; Chou, J. J.; Shih, W. M. DNA-Nanotube-Induced Alignment of Membrane Proteins for NMR Structure Determination. *Proc. Natl. Acad. Sci. U. S. A.* **2007**, *104*, 6644–6648.
22. Lund, K.; Liu, Y.; Lindsay, S.; Yan, H. Self-Assembling a Molecular Pegboard. *J. Am. Chem. Soc.* **2005**, *127*, 17606–17607.
23. Park, S. H.; Pistol, C.; Ahn, S. J.; Reif, J. H.; Lebeck, A. R.; Dwyer, C.; LaBean, T. H. Finite-Size, Fully Addressable DNA Tile Lattices Formed by Hierarchical Assembly Procedures. *Angew. Chem., Int. Ed.* **2006**, *45*, 735–739.
24. Chworos, A.; Severcan, I.; Koyfman, A. Y.; Weinkam, P.; Oroudjev, E.; Hansma, H. G.; Jaeger, L. Building Programmable Jigsaw Puzzles with RNA. *Science* **2004**, *306*, 2068–2072.
25. Endo, M.; Sugita, T.; Katsuda, Y.; Hidaka, K.; Sugiyama, H. Programmed-Assembly System Using DNA Jigsaw Pieces. *Chem.—Eur. J.* **2010**, *16*, 5362–5368.
26. Zhao, Z.; Yan, H.; Liu, Y. A Route to Scale Up DNA Origami Using DNA Tiles as Folding Staples. *Angew. Chem., Int. Ed.* **2010**, *49*, 1414–1417.